IMA Journal of Applied Mathematics (1999) **63**, 89–112

Estimating rate constants in a convection–diffusion system with a boundary reaction

DAVID A. EDWARDS[†]

Department of Mathematics, University of Maryland, College Park, College Park, Maryland 20742-4015*, USA*

[Received 25 September 1997 and in revised form 28 July 1998]

While performing biomolecular interaction analysis (BIA), scientists often use surface plasmon resonance (SPR) to measure rate constants of the associated reactions. A mathematical model of a BIAcore^{TM}, a common SPR device, consists of a convection–diffusion equation in a channel with a reacting surface at the channel ceiling. Asymptotic and singular perturbation techniques are used to analyse the concentration of the reacting species in two cases: when the reaction occurs much more slowly than diffusion, and when the reaction occurs on the same time-scale as diffusion. Linear and nonlinear integral equations result from the analysis; explicit and asymptotic solutions are constructed for physically realizable cases. These expressions provide a direct way to estimate the rate constants from raw data.

1. Introduction

The study of chemical reactions is of great importance to the biological and chemical sciences. Fundamental to the understanding of such reactions are quantitative measurements of the governing *rate constants* in a reaction. Of particular interest in biological applications are bimolecular reactions where one of the reactants is confined to a surface, while the other is immersed in a volume of which the surface is one of the boundaries (Goldstein & Dembo 1995). Thus, the field of biomolecular interaction analysis (BIA) has become quite active.

Surface plasmon resonance (SPR) allows the measurement of rate constants in such surface–volume reactions, and the BIAcore^{TM} is a popular device for performing SPR. The BIAcore^{TM} device consists of a channel through which one of the reactants flows (see Fig. 1). The other reactant, called the receptor, is coupled to a sensor surface on the ceiling of the channel. A polarized light beam reflects off the channel ceiling and passes to a detector. Refractive changes due to the binding of the reactants are then averaged over the length of the ceiling to provide real-time measurement of the bound-state concentration (Karlsson *et al*. 1991; Szabo *et al*. 1995).

The area of surface–volume reactions has great applicability. Receptors confined to the surface of a cell react with ligands floating in the cytoplasm (Goldstein & Dembo 1995). Antigen–antibody interactions occur in such geometries, and gene expression is significantly influenced by DNA–protein interactions. Also, purification processes often

[†]Current Address: Department of Mathematical Sciences, University of Delaware, Newark, Delaware, 19716-2553, USA ⟨edwards@math.udel.edu⟩

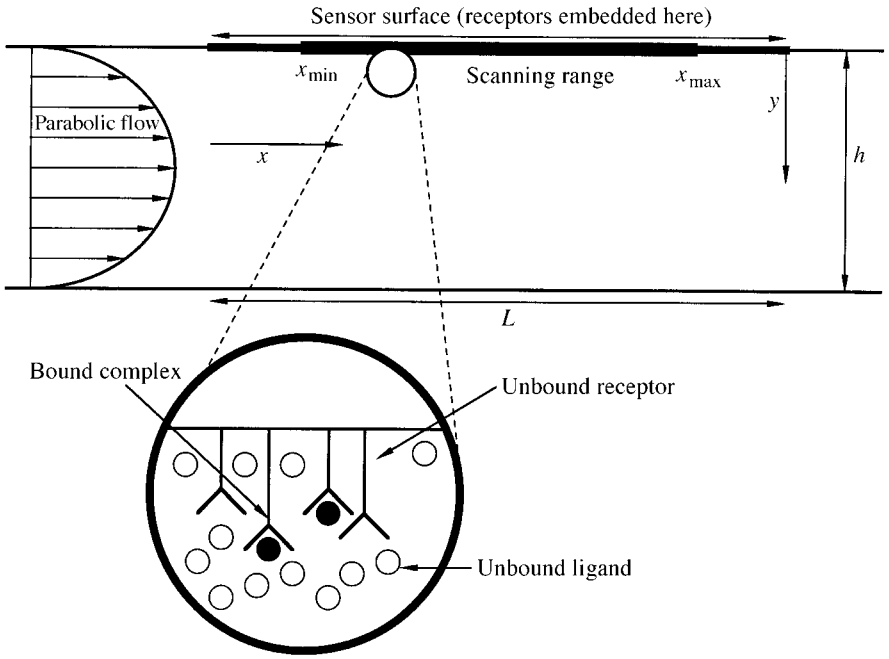

FIG. 1. Schematic of the BIAcore^{TM} device

occur in channels with reactants embedded along a wall, and thus the BIAcore^{TM} is a natural device for analysing the steps in such processes. In all of these cases, the SPR technique has been quite successful in computing rate constants for the associated reactions (Szabo *et al.* 1995; Yarmush *et al.* 1996). Further discussions of the biochemical applications of surface–volume reactions can be found in (Edwards *et al.* forthcoming).

To calculate the rate constants from the raw data, one must model the convection–diffusion system with associated reaction. Though there has been some modeling of all the dynamics in similar systems (Goldstein & Dembo 1995; Lok *et al.* 1983), most authors decouple the reaction kinetics from the transport dynamics. When one decouples the two effects, the equations that result are easily solved in terms of exponentials (Corr *et al.* 1994). Unfortunately, this decoupling occurs only when parameter values are in certain ranges (Karlsson *et al.* 1994). Though there have been numerical simulations that include transport effects (Glaser 1993), few analytical studies have been undertaken.

In this paper, we model the full convection–diffusion system with the reaction at the boundary. Through scaling arguments, we show that there are four distinct time-scales: one each for convection, diffusion near the wall, diffusion into the binding surface, and reaction on the binding surface. The flow away from the walls equilibrates on the convective time-scale, and then the flow near the walls equilibrates on the time-scale of diffusion near the wall. Lastly, the bound concentration evolves on the longer of the remaining two time-scales.

We solve the resulting equations via a perturbation analysis. By using knowledge

about the convective flow, we can reduce the full set of equations to an integrodifferential equation at the boundary. In the case of small Damköhler number (Da) where the kinetics and transport effects decouple, we construct the correction to a previously derived one-term expansion for small Da, thus increasing its range of validity. The form of the regular expansions suggests a multiple-scale expansion, which is also constructed.

Due to the nature of the BIAcore^{TM} device, it is often difficult to set up the experiment such that $\mathrm{Da} = o(1)$. Therefore, we also analyse the system when $\mathrm{Da} = O(1)$ and diffusion and reaction effects balance. A nonlinear integral equation results, but the rate constants can easily be estimated from a short-time solution for the bound-state concentration. In the specialized but physically important case where the bound state is initially a constant, explicit solutions are constructed in terms of known quantities. These solutions provide a direct way to estimate the rate constants not only when $\mathrm{Da} = o(1)$, but also in the previously ignored case when $\mathrm{Da} = O(1)$.

2. Governing equations

The BIAcore^{TM} experimental device can best be modelled as a two-dimensional channel, closed at top and bottom, with height h (see Fig. 1). Unbound ligands flow down the channel in solution, and receptors are attached to a portion of the channel ceiling of length L. The receptors and ligands bind together, and measurements of that bound ligand concentration are taken by computing a quantity averaged over space:

$$\bar{B}(t_c) = \frac{1}{x_{\max} - x_{\min}} \int_{x_{\min}}^{x_{\max}} B(x, t_c)\, \mathrm{d}x, \tag{2.1}$$

where B is the concentration of the bound state, t_c is time, and x is distance along the channel measured from the beginning of the reacting portion. The dimensionless variables B and x are normalized by the total number of receptor sites R_T and by L, respectively. Thus, B represents the proportion of reacting sites actually bound and $x \in [0, 1]$. Here $x_{\min}$ is a finite distance away from 0 and $x_{\max}$ is a finite distance away from 1. We choose the time-scale L/V, where V is a characteristic convective velocity, because it is the fastest scale. (For further discussions of the sizes of all the relevant parameters, see the Appendix.)

Since the Reynolds number is quite small for this system, we expect laminar convective flow. Any perturbations in this flow near $x = 0$ introduced by narrowing of the channel, etc., decay on an $O(\epsilon)$ scale, where $\epsilon = h/L$ is the aspect ratio (Brody *et al.* 1996). Since $0 < \epsilon \ll 1$ and our measurements begin a finite distance away from zero, we may use the standard two-dimensional Poiseuille flow with (adjustable) maximal velocity.

The unbound ligands will also diffuse with molecular diffusion coefficient $\tilde{D}$. Thus, the mathematical model is the following two-dimensional convection–diffusion equation, expressed in dimensionless form:

$$\frac{\partial C}{\partial t_c} = \mathrm{Pe}^{-1}\left(\epsilon^2 \frac{\partial^2 C}{\partial x^2} + \frac{\partial^2 C}{\partial y^2}\right) - y(1-y)\frac{\partial C}{\partial x}, \qquad 0 \leqslant x \leqslant 1, \quad 0 \leqslant y \leqslant 1, \tag{2.2}$$

where C is the concentration of the ligand, y measures distance below the channel ceiling, and $\mathrm{Pe} = Vh^2/\tilde{D}L$ is the Peclét number. The velocities achieved in the BIAcore^{TM} are large compared to the diffusion rate, and hence we take $\mathrm{Pe} \gg 1$.

We have scaled the variable y by h and the concentration has been scaled by an adjustable prescribed inflow concentration C_T. This scaling then implies that

$$C(0, y, t_c) = 1. \tag{2.3}$$

The initial concentration in the channel is known:

$$C(x, y, 0) = C_i(x, y). \tag{2.4}$$

At the downstream end of the channel ($x = 1$), there is no change in the flow concentration:

$$\frac{\partial C}{\partial x}(1, y, t_c) = 0, \tag{2.5}$$

and there is no flux through the channel floor ($y = 1$):

$$\frac{\partial C}{\partial y}(x, 1, t_c) = 0. \tag{2.6}$$

Since there are no other sources or sinks, the flux normal to the binding surface ($y = 0$) must be equal to the rate of change of the bound receptor concentration:

$$\frac{\partial B}{\partial t_c} = D\frac{\partial C}{\partial y}(x, 0, t_c), \qquad D = \frac{\tilde{D}C_T L}{R_T V h}. \tag{2.7a}$$

We note that D may be rewritten as

$$D = \frac{\tilde{D}C_T/R_T h}{V/L} = \frac{\text{diffusion rate from channel to reacting surface}}{\text{convective transport rate in channel}} = \frac{C_T h/R_T}{\text{Pe}}, \tag{2.7b}$$

and that the numerator and denominator in the last expression in (2.7b) can be varied independently of one another in an experimental survey. We note from the Appendix that for physically realizable systems, $D \ll 1$.

The introduction of the new unknown B requires the imposition of another boundary condition, which is given by the evolution of the bimolecular reaction:

$$\frac{\partial B}{\partial t_c} = k_{on}\left[(1 - B)C(x, 0, t_c) - KB\right], \qquad k_{on} = \frac{\tilde{k}_{on}C_T L}{V}, \qquad K = \frac{\tilde{K}}{C_T}, \qquad \tilde{K} = \frac{\tilde{k}_{off}}{\tilde{k}_{on}}. \tag{2.8}$$

Here $\tilde{k}_{on}$ is the *association rate constant*, which measures the speed of the reaction in the presence of both reacting species, $\tilde{k}_{off}$ is the *dissociation rate constant*, which measures the rate of dissociation of the bound state in the absence of the other reactant, the ratio $\tilde{K}$ is the dimensional *equilibrium dissociation constant*, while K is the dimensionless version. Note that k_{on} is the 'natural' dimensionless reaction rate (defined so that the forward reaction takes place on the time-scale $t_c = k_{on}^{-1}$). Lastly, we need an initial condition for B:

$$B(x, 0) = B_i(x). \tag{2.9}$$

3. Preliminaries

3.1 *The steady state*

However complicated the evolution of equations (2.2) to (2.9) may be, important results needed to estimate the rate constants may be obtained simply by solving those equations for their steady states, which we denote by the subscript s. It should be clear from the forms of the boundary data (2.3) and (2.5) to (2.7a) that the steady-state solution for the unbound ligands is $C_s(x, y) = 1$. Substituting this expression into the steady-state form of (2.8) and solving, we obtain

$$B_s(x) = \frac{1}{K+1} = \frac{1}{\alpha}, \qquad \alpha = 1 + K, \tag{3.1a}$$

$$= \frac{C_T}{\tilde{K} + C_T}. \tag{3.1b}$$

Note that the steady-state solutions do *not* depend on the size of Pe and ϵ and also do not depend on the initial data.

From (3.1a) we note that for any experiment, a measurement of the long-time asymptote of $B(x, t)$ will yield a value for K. However, due to normal experimental error, the calculated value for K will be only approximate. By running many experiments to obtain numerous data points, one can perform a linear or nonlinear regression analysis to yield a best estimate for K. For instance, by varying values of C_T and fitting a curve of B_s *vs.* C_T, one can obtain a better estimate for $\tilde{K}$. If we take the ratio of the steady-state bound concentration B_s to the injected concentration of unbound ligands, we have

$$\frac{B_s}{C_T} = \frac{1}{\tilde{K}} - \frac{B_s}{\tilde{K}}. \tag{3.2}$$

Therefore, creating a *Scatchard plot* of B_s/C_T *vs.* B_s for various C_T will yield a straight line with $\tilde{K}$ as the negative reciprocal of the slope (Motulsky 1996).

Unfortunately, considering the steady state gives us only one data point for $\tilde{K}$ per run. In order to get an appropriate estimate for both $\tilde{k}_{on}$ and $\tilde{k}_{off}$, we must have another piece of information, which we shall derive in later sections. In addition, we expect that the rate constants will affect the evolution of B. Therefore, the development of an accurate evolution equation for B will allow us to use real-time measurements as data points for our parameter estimation.

3.2 *The outer solution*

Since the Peclét number is large, we think of Pe^{-1} as a perturbation parameter in the following series:

$$C(x, y, t_c; \mathrm{Pe}) = C_c(x, y, t_c) + o(1), \qquad B(x, t_c; \mathrm{Pe}) = B_c(x, t_c) + o(1). \tag{3.3}$$

Substituting (3.3) into (2.7a) and using the fact that D is small, we obtain

$$\frac{\partial B_c}{\partial t_c} = 0 \tag{3.4a}$$

to leading order. Since the evolution of the bound state is governed by a slower diffusive process, only the unbound ligand concentration will evolve on the t_c time-scale and we have

$$B_c(x, t_c) = B_i(x). \tag{3.4b}$$

If the right-hand side of (2.8) is non-zero, then a boundary layer must be inserted near the reacting surface to enforce consistency with (3.4a), as discussed in Subsection 3.3.

Substituting (3.3) into (2.2) to (2.4) and expanding to leading order, we have the following:

$$\frac{\partial C_c}{\partial t_c} = -y(1-y)\frac{\partial C_c}{\partial x}, \qquad C_c(0, y, t_c) = 1, \qquad C_c(x, y, 0) = C_i(x, y), \tag{3.5}$$

the solution of which is

$$C_c(x, y, t_c) = \begin{cases} C_i\,(x - y(1-y)t_c, y)\,, & \text{if } x - y(1-y)t_c > 0, \\ 1, & \text{otherwise.} \end{cases} \tag{3.6}$$

Since the operator in (3.5) is of lower order than (2.2), its solution (3.6) may not satisfy all the boundary conditions on the full problem. This will necessitate the formation of several boundary and internal layers.

3.3 *Diffusive layers*

We note from (3.4a) that the dynamics of interest, the evolution of the bound state, do not occur on the t_c time-scale. Therefore, any diffusive boundary layers will only be necessary to smooth the discontinuities in the outer solution. Hence we only enumerate them, rather than discuss them in detail.

From (2.6), we see that there will be a layer in the derivative near $y = 1$ if $\partial C_i/\partial y(x, 1) \neq 0$. In addition, there may be a layer near $y = 0$ where the unbound ligand concentration adjusts to (2.8) with $B = B_i$. There may also be a layer about the convective wave front if $C_i(0, y) \neq 1$. All of the diffusive layers on this time-scale are $O(\mathrm{Pe}^{-\frac{1}{2}})$ wide.

Lastly, there is a layer at $x = 1$ caused by the boundary condition (2.5), also of width $O(\mathrm{Pe}^{-\frac{1}{2}})$. However, since measurements of the bound ligand concentration stop at $x_{\max}$, which is an $O(1)$ distance from $x = 1$, we never worry about satisfying equation (2.5). In particular, when convenient we take x to be semi-infinite.

4. Boundary layer with reaction

4.1 *Governing equations*

Since the evolution of B must take place on a long time-scale, we compress t_c by letting $t_D = \mathrm{Pe}^{-\frac{1}{3}} t_c$, where the D indicates the diffusive time-scale. As $t_c \to \infty$, (3.6) approaches 1 everywhere except on the boundaries. Thus, there is a discontinuity at $y = 0$.

To resolve this layer, we stretch y by letting

$$\eta = \mathrm{Pe}^{\frac{1}{3}} y, \qquad C(x, y, t_c) = C_D(x, \eta, t_D), \qquad B(x, t_c) = B_D(x, t_D).$$

This $\mathrm{Pe}^{\frac{1}{3}}$ scaling is common to convection–diffusion–reaction systems of this type (Glaser 1993; Lok *et al.* 1983). Since the characteristic time for diffusion is much greater than that for convection, the effect of the wall has more time to propagate, and hence the boundary layer is wider than those mentioned in Section 3.3.

Substituting these new variables into (2.2), (2.3), (2.7a), (2.8) and (2.9), we have the following, to leading order:

$$\frac{\partial C_D}{\partial t_D} = \frac{\partial^2 C_D}{\partial \eta^2} - \eta \frac{\partial C_D}{\partial x}, \tag{4.1}$$

$$C_D(0, \eta, t_D) = 1, \tag{4.2}$$

$$\frac{\partial B_D}{\partial t_D} = D_D \frac{\partial C_D}{\partial \eta}(x, 0, t_D), \qquad D_D = D\mathrm{Pe}^{\frac{2}{3}} = \frac{C_\mathrm{T} h / R_\mathrm{T}}{\mathrm{Pe}^{\frac{1}{3}}}, \tag{4.3a}$$

$$\frac{\partial B_D}{\partial t_D} = k_\mathrm{on}\mathrm{Pe}^{\frac{1}{3}} \left[(1 - B_D) C_D(x, 0, t_D) - K B_D\right], \tag{4.3b}$$

$$B_D(x, 0) = B_\mathrm{i}(x). \tag{4.4}$$

We note that equation (4.1) has all the salient features of (2.2) with the exception of diffusion in the x-direction, which is $O(\epsilon^2 \mathrm{Pe}^{\frac{1}{3}}) = o(1)$ smaller than the terms in (4.1). The term D_D measures the ratio of the diffusion rate into the surface to the diffusion rate in the boundary layer. Equating the right-hand sides of (4.3), we obtain

$$\frac{\partial C_D}{\partial \eta}(x, 0, t_D) = \mathrm{Da}\left[(1 - B_D) C_D(x, 0, t_D) - K B_D\right], \qquad \mathrm{Da} = \frac{k_\mathrm{on}\mathrm{Pe}^{\frac{1}{3}}}{D_D}, \tag{4.5}$$

where Da is the *Damköhler number*, which measures the ratio of the reaction rate to the diffusion rate in the boundary layer.

In physical terms, our function C_D, which blends the effects of diffusion and convection, must match to the convective solution C_c as we exit the layer. Thus, while the flow away from the walls equilibrates on the t_c time-scale, the flow near the walls equilibrates on the t_D time-scale.

As noted in the Appendix, D_D can be either smaller than $O(1)$. In addition, Da can be larger than, smaller than, or $O(1)$. Therefore, we must break our work up into many cases.

4.2 *Case* 1, $\mathrm{Da} \ll 1$

In this case, the reaction is too slow to use up any diffusive flux, and (4.5) becomes

$$\frac{\partial C_D}{\partial \eta}(x, 0, t_D) = 0. \tag{4.6}$$

Substituting (4.6) into (4.3a), we obtain

$$\frac{\partial B_D}{\partial t_D} = 0 \qquad \Longrightarrow \qquad B_D(x, t_D) = B_\mathrm{i}(x), \tag{4.7}$$

where we have used (4.4). Since this time-scale is faster than the one on which the bound concentration changes, this boundary layer captures only the slow diffusion near the wall. The system governing the evolution of the unbound ligand concentration is given by (4.1), (4.2) and (4.6).

Since the evolution of the bound state occurs on a slower time-scale than t_D, we introduce the following new variables:

$$t = k_{\mathrm{on}}\mathrm{Pe}^{\frac{1}{3}} t_D = k_{\mathrm{on}} t_{\mathrm{c}} = \tilde{k}_{\mathrm{on}} C_{\mathrm{T}} \tilde{t}, \tag{4.8a}$$

$$C_D(x, \eta, t_D) = C_k(x, \eta, t) + o(1), \qquad B_D(x, t_D) = B_k(x, t) + o(1), \tag{4.8b}$$

where $\tilde{t}$ is the dimensional time-scale. In (4.8a), $k_{\mathrm{on}}\mathrm{Pe}^{\frac{1}{3}}$ is small because D_D is never larger than $O(1)$ and their ratio $k_{\mathrm{on}}\mathrm{Pe}^{\frac{1}{3}}/D_D = \mathrm{Da} \ll 1$. Substituting (4.8) into (4.3b), we obtain

$$\frac{\partial B_k}{\partial t} = (1 - B_k) C_k(x, 0, t) - K B_k, \tag{4.9}$$

and thus t is the time-scale on which the reaction occurs.

Substituting (4.8) into (4.1), (4.2) and (4.4), we have the following, to leading order:

$$\eta \frac{\partial C_k}{\partial x} = \frac{\partial^2 C_k}{\partial \eta^2}, \tag{4.10}$$

$$C_k(0, \eta, t) = 1, \tag{4.11}$$

$$B_k(x, 0) = B_{\mathrm{i}}(x). \tag{4.12}$$

The appropriate similarity variable for (4.10) is $\eta/x^{\frac{1}{3}}$, and hence the effects of diffusion will become more pronounced with increasing x (Karlsson *et al.* 1994). Substituting (4.8) into (4.3a) to obtain the other boundary condition at the reacting surface, we obtain

$$\frac{\partial C_k}{\partial \eta}(x, 0, t) = \mathrm{Da} \frac{\partial B_k}{\partial t}, \tag{4.13a}$$

which becomes

$$\frac{\partial C_k}{\partial \eta}(x, 0, t) = 0 \tag{4.13b}$$

in the limit of small Da. In order to match C_k to the uniform outer solution, we require that

$$C_k(x, \infty, t) = 1. \tag{4.14}$$

We note that B_k will depend on K and t, which itself depends on k_{on}. Therefore, by taking measurements of $\bar{B}_k$ and comparing the results with our solutions, we should be able to obtain good estimates for K and k_{on}. Since C_{T} is known for each experiment, one can easily estimate $\tilde{k}_{\mathrm{on}}$ and $\tilde{k}_{\mathrm{off}}$, which is the end goal of this process.

At least to leading order, the solutions of the equations for this case are well known (Corr *et al.* 1994). They are easy to solve (as we shall show in Subsection 5.1) because the transport effects are divorced from the reaction kinetics. Therefore, it is the goal of

biochemists to set up their experimental apparatus such that these two dynamical processes occur on disparate scales. It is clear from this analysis that in order to do so, they must set

$$\mathrm{Da} \ll 1 \qquad \Longrightarrow \qquad V \gg \frac{\tilde{k}_{\mathrm{on}}^3 R_{\mathrm{T}}^3 h L}{\tilde{D}^2}, \tag{4.15}$$

as in Karlsson *et al.* (1994). Of course, one must estimate the magnitude of $\tilde{k}_{\mathrm{on}}$ in order to estimate the threshold value of V. In practice, experimentalists simply increase V until the data from the apparatus matches the leading-order theoretical predictions.

Unfortunately, in order to get measurable readings from the detector, a large number of receptor sites is needed. Since the bound for V depends on the cube of R_{T}, R_{T} is often so large that the velocity cannot be increased enough to make $\mathrm{Da} = o(1)$.

4.3 *Case* 2: $\mathrm{Da} \gg 1$

In this case, the reaction is so fast that the unbound ligand concentration must adjust to the proper concentration at the surface, and (4.5) becomes, to leading order,

$$C_D(x, 0, t_D) = \frac{K B_D}{1 - B_D}. \tag{4.16}$$

Unfortunately, in this case the leading-order solutions depend only on K, not the individual rate constants. Thus, we cannot obtain the rate constants separately with leading-order solutions alone. Happily, this case does not occur often in practice, as experimentalists can often increase the velocity enough to make $\mathrm{Da} = O(1)$.

Case 2a: $\mathrm{Da} \gg 1$, $D_D \ll 1$. In this case, the evolution of the bound concentration at the surface must take place on a slower time-scale. A dominant balance is obtained when we let

$$t_{\mathrm{w}} = D_D t_D = D_D \mathrm{Pe}^{-\frac{1}{3}} t_{\mathrm{c}}, \qquad C_D(x, \eta, t_D) = C_{\mathrm{w}}(x, \eta, t_{\mathrm{w}}), \qquad B_D(x, t_D) = B_{\mathrm{w}}(x, t_{\mathrm{w}}), \tag{4.17}$$

where the subscript w indicates that wall dynamics are important in this region. Substituting (4.17) into (4.1), (4.2), (4.4) and (4.3b), we obtain (4.10) to (4.12) and (4.16) with the subscripts k and D replaced by w. The matching condition (4.14) also holds with the switched subscripts. Substituting (4.17) into (4.3a), we have the final boundary condition:

$$\frac{\partial B_{\mathrm{w}}}{\partial t_{\mathrm{w}}} = \frac{\partial C_{\mathrm{w}}}{\partial \eta}(x, 0, t_{\mathrm{w}}). \tag{4.18}$$

Case 2b: $\mathrm{Da} \gg 1$, $D_D = O(1)$. In this case, we see that the following are true.

(1) We must use the full form of (4.3a) as a boundary condition for the evolution on the t_D time-scale.

(2) Since $D_D = O(1)$, t_D and t_{w} are of the same order. Thus, the solution of both bound and unbound ligand concentration evolves on the t_D time-scale as governed by (4.1) to (4.3a), (4.4) and (4.16).

4.4 *Case* 3: Da $= O(1)$

In this case, the reaction rate balances with the diffusion process, and thus (4.5) cannot be reduced. However, t_w and t are now of the same order, so we may write our leading-order solutions in terms of t and K which, as indicated before, will allow us to calculate both rate constants. Once again, there are two subcases to consider, depending on the size of D_D.

Case 3a: Da $= O(1)$, $D_D \ll 1$. On the t_D time-scale, (4.3a) reduces to the form in (4.7) since $D_D \ll 1$. Upon substituting $B_D = B_i$ into (4.5), we obtain

$$\frac{\partial C_D}{\partial \eta}(x, 0, t_D) = \mathrm{Da}\,[(1 - B_i)C_D(x, 0, t_D) - K B_i]\,. \tag{4.19}$$

Thus, evolution on the t_D time-scale is governed by (4.1), (4.2) and (4.19). On the t time-scale, we may proceed as in case 1, with (4.13b) replaced by (4.13a) for the proper boundary condition since Da $= O(1)$. Therefore, evolution on the t scale is governed by (4.9) to (4.13a) and (4.14).

Case 3b: Da $= O(1)$, $D_D = O(1)$. Both of our parameters are $O(1)$ in this case, so t_D, t_w, and t are all of the same order. Thus, we must work with the full system on the t_D time-scale, which is given by (4.1) to (4.5).

4.5 *Summary*

Since Pe $\gg 1$, the flow away from the walls equilibrates on the convective time-scale (subscripts c), and then the flow near the walls equilibrates on the diffusive time-scale (subscripts D), which is $\mathrm{Pe}^{\frac{1}{3}}$ longer. The remaining two time-scales are the reaction time-scale (subscripts k), which is k_{on}^{-1} longer than the convective time-scale, and the time-scale for diffusion into the ceiling (subscripts w), which is $\mathrm{Pe}^{\frac{1}{3}}/D_D$ longer than the convection time-scale. The bound concentration evolves on the longer of these latter two. If Da $= O(1)$, then these two time-scales are of the same order. If $D_D = O(1)$, then diffusion in the boundary layer and diffusion into the ceiling occur on the same time-scale.

5. Asymptotic solution of case 1, Da $\ll 1$, $D_D \ll 1$

As previously mentioned, experimentalists attempt to operate in the regime of small Da (case 1), since the leading-order behaviour of the bound concentration is easy to deduce (Corr *et al.* 1994). We shall calculate the first *two* terms of the expansion for the bound concentration in the limit of small Da. This additional term should allow us to increase the range of Da for which our expansion is a good approximation.

As noted in the Appendix, though D_D can be $O(1)$, in almost all physically realizable cases, $D_D \ll 1$. Therefore, we reduce to that subcase in this section. Such a choice affects only the correction to the leading-order solution, as indicated below. Since the receptors can initially be laid down at a variable concentration, we consider the case of general $B_i(x)$. However, the most common case is B_i constant, which we address in Subsections 5.3 and 6.2.

5.1 *Regular expansion*

In order to calculate the next term in a perturbation expansion, we must determine the proper perturbation parameter. It is not appropriate to use Pe^{-1}, since convective effects are subdominant in this regime. The two possible choices are $k_{\mathrm{on}}\mathrm{Pe}^{\frac{1}{3}}$, which arises from the time-derivative term in the full form of equation (4.1), and Da, which arises from (4.13a). Since the ratio $k_{\mathrm{on}}\mathrm{Pe}^{\frac{1}{3}}/\mathrm{Da} = D_D \ll 1$, Da is the larger parameter and so we use Da for the perturbation parameter. Hence our expansions become

$$C_k(x, \eta, t) = C_0(x, \eta, t) + \mathrm{Da}C_1(x, \eta, t) + o(\mathrm{Da}), \tag{5.1a}$$

$$B_k(x, t) = B_0(x, t) + \mathrm{Da}B_1(x, t) + o(\mathrm{Da}). \tag{5.1b}$$

Substituting (5.1) into (4.9) to (4.13a) and (4.14), the leading order is given by (4.9) to (4.12), (4.13b) and (4.14) with the subscript k replaced by the subscript 0. At the next order, we have

$$\eta \frac{\partial C_1}{\partial x} = \frac{\partial^2 C_1}{\partial \eta^2}, \tag{5.2a}$$

$$C_1(0, \eta, t) = 0, \qquad C_1(x, \infty, t) = 0, \tag{5.2b}$$

$$\frac{\partial C_1}{\partial \eta}(x, 0, t) = \frac{\partial B_0}{\partial t}, \tag{5.3}$$

$$\frac{\partial B_1}{\partial t} = (1 - B_0)C_1(x, 0, t) - B_1 C_0(x, 0, t) - K B_1, \tag{5.4}$$

$$B_1(x, 0) = 0. \tag{5.5}$$

If we had chosen $D_D = O(1)$, equation (5.2a) would also have included a term of the form $\partial C_0/\partial t$.

Upon inspection, the solution of the leading-order equations is found to be

$$C_0(x, \eta, t) = 1. \tag{5.6}$$

Substituting (5.6) into the new form of (4.9), we obtain the evolution equation

$$\frac{\partial B_0}{\partial t} = 1 - \alpha B_0. \tag{5.7}$$

Before solving (5.7), we note that if we take its mean (in the sense of (2.1)) and then write most of the quantities in dimensional form, we have the following:

$$\frac{\mathrm{d}\bar{B}_0}{\mathrm{d}\tilde{t}} = \tilde{k}_{\mathrm{on}} C_{\mathrm{T}} - S\bar{B}_0, \qquad S = \tilde{k}_{\mathrm{on}} C_{\mathrm{T}} + \tilde{k}_{\mathrm{off}}, \tag{5.8}$$

where we have used the definitions in (2.8) and (4.8a). Therefore, a plot of $\mathrm{d}\bar{B}_0/\mathrm{d}\tilde{t}$ *vs.* $\bar{B}_0$ will yield a straight line with slope S. Since C_{T} is a known quantity which can be varied in different experiments, a plot of S *vs.* C_{T} will be a straight line with slope $\tilde{k}_{\mathrm{on}}$ and intercept $\tilde{k}_{\mathrm{off}}$. It is in this way that rate constants are often calculated with the BIAcore$^{\mathrm{TM}}$ device (Glaser 1993; Karlsson *et al.* 1991). Note also that due to the special form of (5.8), we do not use the steady-state solution (3.1a) to provide information about K.

Solving (5.7) subject to the new form of (4.12), we obtain

$$B_0(x,t) = \frac{1-\mathrm{e}^{-\alpha t}}{\alpha} + B_\mathrm{i}(x)\mathrm{e}^{-\alpha t}, \tag{5.9a}$$

$$\bar{B}_0(t) = \frac{1-\mathrm{e}^{-\alpha t}}{\alpha} + \bar{B}_\mathrm{i}\mathrm{e}^{-\alpha t}. \tag{5.9b}$$

Unfortunately, due to the large size of R_T in a typical experiment, Da often becomes large enough that a leading-order expansion is not good enough to provide meaningful estimates. Therefore, we continue by constructing the next order in the perturbation expansion.

Substituting (5.6) into (5.4) and solving for $C_1(x,0,t)$, we have the following:

$$C_1(x,0,t) = \frac{1}{1-B_0}\left(\frac{\partial B_1}{\partial t} + B_1 + KB_1\right). \tag{5.10}$$

To obtain a solution, we introduce a Laplace transform in x into (5.2a) and (5.10) subject to (5.2b). The solution of the transformed equations is an Airy function whose derivative at $\eta = 0$ can be readily computed. We then substitute this result into the Laplace transform of (5.3). The resulting expression may be manipulated and inverted to yield

$$\frac{1}{1-B_0}\left(\frac{\partial B_1}{\partial t} + B_1 + KB_1\right) = -\frac{1}{3^{\frac{1}{3}}\Gamma(\frac{2}{3})}\int_0^x \frac{\partial B_0}{\partial t}(x-\xi,t)\frac{\mathrm{d}\xi}{\xi^{\frac{2}{3}}}. \tag{5.11}$$

Substituting our form for B_0 from (5.9a) into (5.11) and solving the resulting equation subject to (5.5), we obtain

$$B_1(x,t) = \frac{\mathrm{e}^{-\alpha t}}{3^{\frac{1}{3}}\Gamma(\frac{2}{3})}\left\{\frac{\mathrm{e}^{-\alpha t}-1}{\alpha}\left[\frac{1}{\alpha} - B_\mathrm{i}(x)\right] - \frac{tK}{\alpha}\right\}\left[3x^{\frac{1}{3}} - \alpha\int_0^x \frac{B_\mathrm{i}(x-\xi)}{\xi^{\frac{2}{3}}}\,\mathrm{d}\xi\right]. \tag{5.12}$$

Unfortunately, when we expand (5.12) for large t, a secular term of the form $t\mathrm{e}^{-\alpha t}$ appears. Though $\mathrm{Da}B_1 \ll B_0$ for all t since B_0 approaches an $O(1)$ steady state, this term is troublesome, since upon subtracting the steady state, we obtain $\mathrm{Da}B_1 = O(B_0 - B_\mathrm{s})$ for $t = O(\mathrm{Da}^{-1})$. Therefore, a multiple-scale expansion is desirable, and hence we should use (5.12) as an aid in determining the rate constants only when $t = o(\mathrm{Da}^{-1})$.

The multiple-scale expansion we construct in Subsection 5.2, though mathematically sound, will not provide illuminating physical results. Thus, we construct the next-order correction to our barred quantity, keeping in mind that we should use this expression only for $t = o(\mathrm{Da}^{-1})$:

$$\bar{B}_1(t) = \frac{\mathcal{I}[B_1; x_\mathrm{max}] - \mathcal{I}[B_1; x_\mathrm{min}]}{x_\mathrm{max} - x_\mathrm{min}}, \qquad \mathcal{I}[f;x] = \int_0^x f(\xi)\,\mathrm{d}\xi, \tag{5.13}$$

where

$$\mathcal{I}[B_1;x] = \frac{3^{\frac{2}{3}}\mathrm{e}^{-\alpha t}}{\Gamma(\frac{2}{3})}\left(\frac{\mathrm{e}^{-\alpha t}-1}{\alpha^2} - \frac{tK}{\alpha}\right)\left[\frac{3x^{4/3}}{4} - \alpha\int_0^x B_\mathrm{i}(x-\xi)\xi^{\frac{1}{3}}\,\mathrm{d}\xi\right]$$
$$+\frac{\mathrm{e}^{-\alpha t}\left(1-\mathrm{e}^{-\alpha t}\right)}{3^{\frac{1}{3}}\alpha\Gamma(\frac{2}{3})}\int_0^x B_\mathrm{i}(\xi)\left[3\xi^{\frac{1}{3}} - \alpha\int_0^\xi \frac{B_\mathrm{i}(\xi-u)}{u^{\frac{2}{3}}}\,du\right]\mathrm{d}\xi. \tag{5.14}$$

5.2 *Multiple-scale expansion*

Since the secularity in our expression occurs at the first order, we introduce the new variables

$$\tau = \mathrm{Da}t, \qquad T = \left(1 + \sum_{n=2}^{\infty} \omega_n \mathrm{Da}^n\right) t, \tag{5.15}$$

and write our dependent variables in the following way:

$$C_k(x, \eta, t) = c_0(x, \eta, \tau, T) + \mathrm{Da}c_1(x, \eta, \tau, T) + o(\mathrm{Da}), \tag{5.16a}$$

$$B_k(x, t) = b_0(x, \tau, T) + \mathrm{Da}b_1(x, \tau, T) + o(\mathrm{Da}). \tag{5.16b}$$

In order to construct the proper equations, we substitute the new variables from (5.15) and (5.16) into (4.9) to (4.13a) and (4.14). At leading order, the governing equations are given by (4.9) to (4.12), (4.13b) and (4.14) with C_k replaced by c_0, B_k replaced by b_0, and t replaced by T. Therefore, the leading-order solution for the concentration field is $c_0(x, \eta, \tau, T) = 1$, as before. Hence we obtain (5.7) with B_0 replaced by b_0 and t replaced by T, the solution of which is given by

$$b_0(x, \tau, T) = \frac{1}{\alpha} + a(x, \tau)\mathrm{e}^{-\alpha T}, \qquad a(x, 0) = B_{\mathrm{i}}(x) - \frac{1}{\alpha}, \tag{5.17}$$

where we have used the new form of (4.12).

The next order of equations (4.10) to (4.13a) and (4.14) is given by (5.2), (5.3), and (5.5) with C_1 replaced by c_1, B_1 replaced by b_1, and t replaced by T. Upon substitution of (5.17), we see that the next order of (4.9) is given by

$$c_1(x, 0, \tau, T) = \frac{1}{1 - b_0}\left(\frac{\partial b_1}{\partial T} + \frac{\partial b_0}{\partial \tau} + b_1 + Kb_1\right), \tag{5.18}$$

which is analogous to (5.10) except for the extra $\partial b_0/\partial\tau$ term arising from the multiple-scale expansion. Thus, to construct the solution for a, we need only the analogue of (5.11), which is

$$\frac{1}{1 - b_0}\left(\frac{\partial b_1}{\partial T} + \frac{\partial b_0}{\partial \tau} + b_1 + Kb_1\right) = -\frac{1}{3^{\frac{1}{3}}\Gamma(\frac{2}{3})}\int_0^x \frac{\partial b_0}{\partial T}(x - \xi, \tau, T)\frac{\mathrm{d}\xi}{\xi^{\frac{2}{3}}}. \tag{5.19}$$

Substituting our expression for b_0 into (5.19), we have

$$\frac{\partial b_1}{\partial T} + \alpha b_1 = \mathrm{e}^{-\alpha T}\left[-\frac{\partial a}{\partial \tau} + \frac{K}{3^{\frac{1}{3}}\Gamma(\frac{2}{3})}\int_0^x \frac{a(x - \xi, \tau)}{\xi^{\frac{2}{3}}}\,\mathrm{d}\xi\right] + \ldots,$$

where the unlisted terms do not contribute to the secularity. To suppress it, we once again introduce a Laplace transform in x. The resulting solution for the transform of a is an exponential which cannot be inverted in closed form. However, we may use the Taylor series for the exponential and invert term-by-term to yield

$$a(x, \tau) = B_{\mathrm{i}}(x) - \frac{1}{\alpha}\sum_{n=0}^{\infty}\frac{(r\tau x^{\frac{1}{3}})^n}{\Gamma(1 + n/3)n!} + \sum_{n=1}^{\infty}\frac{(r\tau)^n}{\Gamma(n/3)n!}\int_0^x \xi^{-1+n/3}B_{\mathrm{i}}(x - \xi)\,\mathrm{d}\xi, \tag{5.20a}$$

$$r = \frac{\Gamma(\frac{1}{3})K}{3^{\frac{1}{3}}\Gamma(\frac{2}{3})}. \tag{5.20b}$$

Though (5.20a) grows exponentially in τ, the $e^{-\alpha t}$ contribution from (5.17) will swamp the $O(e^{Dat})$ contribution from (5.20a) as $t \to \infty$, and hence the expression for b_0 will converge.

In order to obtain estimates for the rate constants, we need the expression for the mean, which is easily found using (5.17):

$$\bar{b}_0(\tau, T) = \frac{1}{\alpha} + \frac{\mathcal{I}[a; x_{\max}] - \mathcal{I}[a; x_{\min}]}{x_{\max} - x_{\min}} e^{-\alpha T}, \tag{5.21}$$

where

$$\mathcal{I}[a; x] = -\frac{x}{\alpha} \sum_{n=0}^{\infty} \frac{(r\tau x^{\frac{1}{3}})^n}{\Gamma(2 + n/3)n!} + \sum_{n=0}^{\infty} \frac{(r\tau)^n}{\Gamma(1 + n/3)n!} \int_0^x \xi^{n/3} B_i(x - \xi)\, d\xi. \tag{5.22}$$

Due to the complicated nature of (5.22), it is best to revert to the expressions given in Subsection 5.1 when actually calculating parameter values. We run the experiment to a steady state, and use (3.1a) to give us an estimate for K. Then we fit the data for $t = o(Da^{-1})$ with the first two terms of the expansion given by (5.9b) and (5.13). From the dependence on t, we can calculate $\tilde{k}_{on}$. Then using the values for K and C_T, we may calculate $\tilde{k}_{off}$.

5.3 *Constant initial state*

Obviously the integral in (5.12) is not amenable to easy calculation for arbitrary $B_i(x)$. Fortunately, in real experiments it is easy (and often convenient) to set up the apparatus such that $B_i(x)$ is a constant value B_i.

In this case, equations (5.9) become

$$B_0(x, t) = \frac{1 - \chi e^{-\alpha t}}{\alpha} = \bar{B}_0(t), \qquad \chi = 1 - \alpha B_i. \tag{5.23}$$

In addition, (5.12) becomes the following:

$$B_1(x, t) = \frac{3^{\frac{2}{3}} x^{\frac{1}{3}} \chi e^{-\alpha t}}{\alpha \Gamma(\frac{2}{3})} \left[\frac{\chi(e^{-\alpha t} - 1)}{\alpha} - Kt \right]. \tag{5.24}$$

Equation (5.14) becomes

$$\mathcal{I}[B_1; x] = \frac{3^{\frac{5}{3}} x^{\frac{4}{3}} \chi e^{-\alpha t}}{4\Gamma(\frac{2}{3})\alpha} \left[\frac{\chi(e^{-\alpha t} - 1)}{\alpha} - Kt \right]. \tag{5.25}$$

Substituting (5.25) into (5.13), we obtain

$$\bar{B}_1(t) = \frac{3^{\frac{5}{3}}(x_{\max}^{\frac{4}{3}} - x_{\min}^{\frac{4}{3}}) \chi e^{-\alpha t}}{4\Gamma(\frac{2}{3})\alpha(x_{\min} - x_{\max})} \left[\frac{\chi(e^{-\alpha t} - 1)}{\alpha} - Kt \right]. \tag{5.26}$$

TABLE 1
Parameter values for Figs 2 and 3

Necessary parameters

Given		*Calculated*	
Parameter	Value	Parameter	Value
B_{i}	0	r	1·37
C_{T} (mol/cm^3)	10^{-11}	T	$10^{-3}\,\tilde{t}$/s
Da	10^{-1}	t	$10^{-3}\,\tilde{t}$/s
K	1	α	2
$\tilde{k}_{\mathrm{on}}$ (cm^{3}mol^{-1}s^{-1})	10^8	τ	$10^{-4}\,\tilde{t}$/s
$x_{\max}$	$7{\cdot}92 \times 10^{-1}$	χ	1
$x_{\min}$	$2{\cdot}08 \times 10^{-1}$		

Ancillary parameters

Given		*Calculated*	
Parameter	Value	Parameter	Value
$\tilde{D}$ (cm^2/s)	$2{\cdot}8 \times 10^{-7}$	D	$3{\cdot}34 \times 10^{-4}$
h (cm)	5×10^{-3}	D_D	$1{\cdot}73 \times 10^{-2}$
Pe	$3{\cdot}71 \times 10^2$	$\tilde{k}_{\mathrm{off}}$ (s^{-1})	10^{-3}
ϵ	$2{\cdot}08 \times 10^{-2}$	R_{T} (mol/cm^2)	$4{\cdot}03 \times 10^{-13}$

Thus, we now have all the component parts necessary to obtain rate constant estimates from the two-term regular perturbation expansion.

The multiple-scale expansion also simplifies greatly. With our choice of $B_{\mathrm{i}}(x)$, (5.22) becomes

$$\mathcal{I}[a; x] = -\frac{\chi x}{\alpha} \sum_{n=0}^{\infty} \frac{(r\tau x^{\frac{1}{3}})^n}{\Gamma(2 + n/3)n!}. \tag{5.27}$$

In order to plot graphs of our solutions, we select parameters motivated by the Appendix. These parameters appear in Table 1. The first half of the table lists the parameters necessary to construct Figs 2 and 3. The physical parameters taken from the Appendix are listed on the left; any parameters calculated from those values are listed on the right. The second half of the table lists other parameters associated with the problem. We note that $D_D \ll 1$, as expected.

Figure 2 shows a graph of $\bar{B}_0$ (as given by (5.23)) versus the *dimensional* time $\tilde{t}$ (in seconds), since this is how the constants would be determined in a given experiment. Also indicated on the graph of Fig. 2 is the long-time asymptote $\alpha^{-1} = \frac{1}{2}$ given by (3.1a). Figure 3 illustrates the differences between the regular and multiple-scale expansions. The solid line is a graph of $\mathrm{Da}\bar{B}_1$ as given by (5.26). The dashed line is a graph of $\bar{B}_0 - \bar{b}_0$, which we calculate by using the first six terms of (5.27) in (5.21).

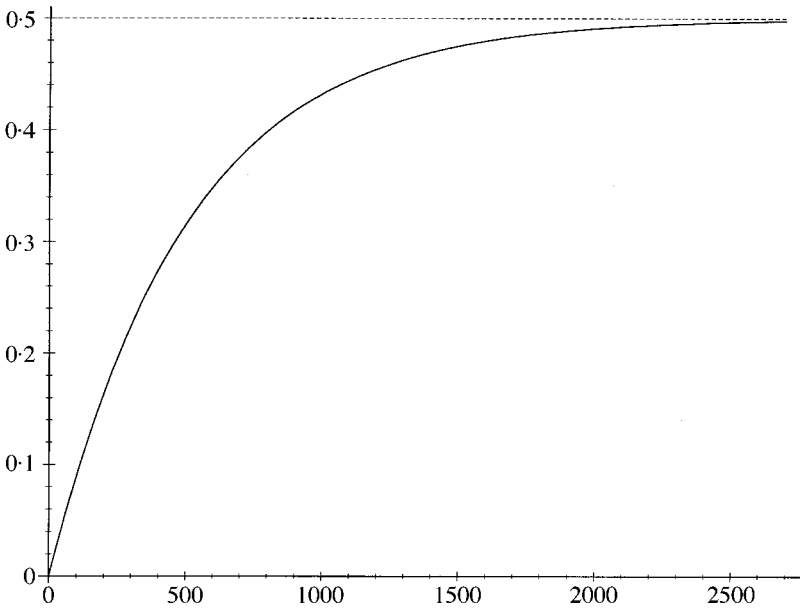

FIG. 2. $\bar{B}_0(\tilde{t})$ *vs.* $\tilde{t}$ for the parameters in Table 1, along with the asymptote $\alpha^{-1} = \frac{1}{2}$

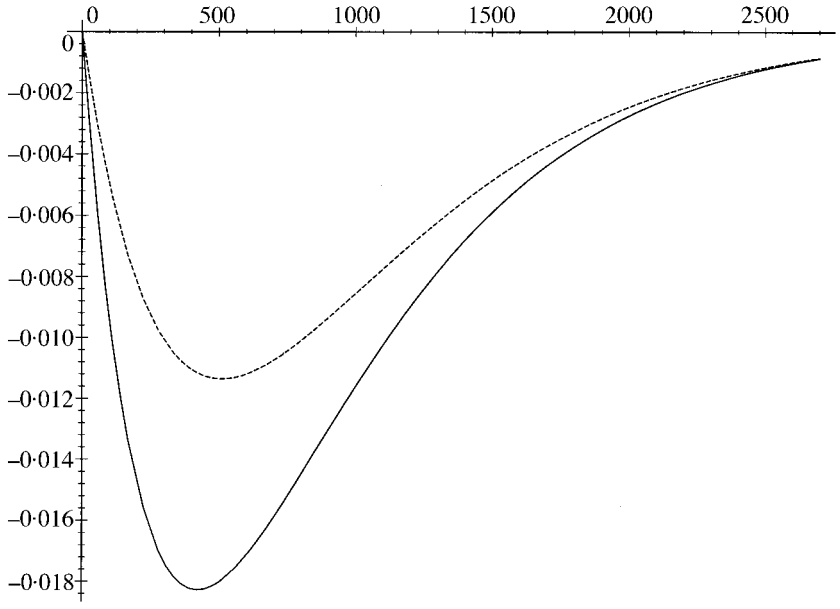

FIG. 3. Correction to $\bar{B}_0(\tilde{t})$ from $\bar{B}_1(\tilde{t})$ (solid line) and $\bar{b}_0(\tilde{t})$ (dashed line) *vs.* $\tilde{t}$ for the parameters in Table 1

6. Case 3a

6.1 *General asymptotic solution*

As indicated before, the other case of real physical significance is the one in which Da $=$ $O(1)$ and $D_D \ll 1$ (case 3a). We wish to obtain an expression for the concentration of the bound ligand state, so we focus on the evolution on the t time-scale. We note that if we rewrite equations (4.9) to (4.11), (4.13a) and (4.14) using $C_1 = 1 - C_k$, we obtain the following correspondences:

(4.10) $\Leftrightarrow$ (5.2a); (4.11), (4.14) $\Leftrightarrow$ (5.2b); (4.13a) $\Leftrightarrow$ (5.3); (4.9) $\Leftrightarrow$ (5.10).

These are not exact correspondences, but the forms of the operators and boundary conditions are the same. Therefore, the solution process is analogous to the one for C_1 in Subsection 5.1. In this case, (5.11) is replaced by

$$1 - \frac{1}{1 - B_k}\left(\frac{\partial B_k}{\partial t} + K B_k\right) = \frac{\mathrm{Da}}{3^{\frac{1}{3}}\Gamma(\frac{2}{3})}\int_0^x \frac{\partial B_k}{\partial t}(x - \xi, t)\frac{\mathrm{d}\xi}{\xi^{\frac{2}{3}}}, \tag{6.1}$$

which is a variant of an Abel equation. In the limit that Da $\to$ 0, (6.1) reduces to the evolution equation (5.7) for B_0, as expected. Of course, (5.7) is exactly the evolution equation for the solution $C_k = 1$, which is what one would expect the unbound ligand concentration to be in the limit of small Da.

In contrast to (5.11), equation (6.1) is nonlinear and is thus very difficult to solve in closed form. However, in order to obtain estimates for the rate constants, we do not need the full solution for B_k. Let us assume a solution of the form

$$B_k(x, t) = B_{\mathrm{i}}(x) + \beta_1(x)t + o(t), \quad t \to 0. \tag{6.2}$$

Once we have calculated β_1 and taken its average, we will obtain an expression that can be compared to the short-time behaviour of the experimental data. Since the result will depend on both K and t, we can then back out the corresponding rate constants.

Substituting the first two orders of (6.2) into (6.1), we have

$$1 - B_{\mathrm{i}}(x) - [\beta_1 + K B_{\mathrm{i}}(x)] = \frac{\mathrm{Da}[1 - B_{\mathrm{i}}(x)]}{3^{\frac{1}{3}}\Gamma(\frac{2}{3})}\int_0^x \frac{\beta_1(x - \xi)}{\xi^{\frac{2}{3}}}\,\mathrm{d}\xi, \tag{6.3}$$

which is again an unwieldy equation. However, this one is more easily solvable since it is linear.

6.2 *Constant initial state*

Following the motivation in Subsection 5.3, we now consider B_{i} to be a constant. In this case, equation (6.3) becomes

$$1 - \alpha B_{\mathrm{i}} - \beta_1 = \frac{\mathrm{Da}(1 - B_{\mathrm{i}})}{3^{\frac{1}{3}}\Gamma(\frac{2}{3})}\int_0^x \frac{\beta_1(x - \xi)}{\xi^{\frac{2}{3}}}\,\mathrm{d}\xi. \tag{6.4}$$

We could solve for β_1 directly, but we really wish to calculate $\bar{B}_k(t)$, which for small t is given by

$$\bar{B}_k(t) = B_\mathrm{i} + \frac{t\{\mathcal{I}[\beta_1; x_\mathrm{max}] - \mathcal{I}[\beta_1; x_\mathrm{min}]\}}{x_\mathrm{max} - x_\mathrm{min}} + o(t), \tag{6.5}$$

where we have used our hypothesis for $B_\mathrm{i}(x)$. Hence, it is more convenient to solve for $\mathcal{I}[\beta_1; x]$. Using Laplace transforms in x, the solution is found to be

$$\mathcal{I}[\beta_1; x] = \frac{\chi \mathrm{e}^{-\mu x}}{\mu}\left[\mathrm{e}^{\mu x} - 1 - |P(\tfrac{4}{3}, -\mu x)| + |P(\tfrac{5}{3}, -\mu x)|\right],$$

$$\mu = \frac{1}{3}\left[\frac{\mathrm{Da}(1 - B_\mathrm{i})\Gamma(\frac{1}{3})}{\Gamma(\frac{2}{3})}\right]^3, \tag{6.6}$$

where P is the normalized incomplete gamma function defined by

$$P(n/3, -\mu x) = \frac{\gamma(n/3, -\mu x)}{\Gamma(n/3)} = \frac{1}{\Gamma(n/3)}\int_0^{-\mu x} \mathrm{e}^{-\xi}\xi^{n/3-1}\,\mathrm{d}\xi.$$

Equation (6.5) is most useful when expressed in dimensional terms:

$$\bar{B}_k(\tilde{t}) \sim B_\mathrm{i} + \frac{\tilde{k}_\mathrm{on} C_\mathrm{T}\tilde{t}\{\mathcal{I}[\beta_1; x_\mathrm{max}] - \mathcal{I}[\beta_1; x_\mathrm{min}]\}}{x_\mathrm{max} - x_\mathrm{min}}, \quad \tilde{t} \to 0, \tag{6.7}$$

where we have used (4.8a). In order to calculate the rate constants, we perform the experiment with B_i constant. We use (3.1a) to obtain an estimate for K from the steady state. In order to calculate both rate constants, we construct a linear fit to our small-time experimental data. Once we have calculated the slope S of that line, we solve the following equation:

$$S = \frac{\tilde{k}_\mathrm{on} C_\mathrm{T}\{\mathcal{I}[\beta_1; x_\mathrm{max}] - \mathcal{I}[\beta_1; x_\mathrm{min}]\}}{x_\mathrm{max} - x_\mathrm{min}} \tag{6.8}$$

to obtain $\tilde{k}_\mathrm{on}$. It is important to note that the relationship between S and $\tilde{k}_\mathrm{on}$ is not linear, since β_1 also depends on $\tilde{k}_\mathrm{on}$ through the parameter Da. Then using our value for K, we may calculate $\tilde{k}_\mathrm{off}$.

In order to determine how S varies with $\tilde{k}_\mathrm{on}$, we select parameters motivated by the Appendix. These parameters appear in Table 2, the layout of which is the same as Table 1. Here the dimensionless rate constant is given by

$$k = 10^{-9}\tilde{k}_\mathrm{on}\frac{\mathrm{mol}\cdot\mathrm{s}}{\mathrm{cm}^3}. \tag{6.9}$$

Substituting our parameters in Table 2 and (6.9) into (6.8), we obtain

$$S = 7{\cdot}2 \times 10^{-2} k\{\mathcal{I}[\beta_1; 0{\cdot}8] - \mathcal{I}[\beta_1; 0{\cdot}2]\}\ \mathrm{s}^{-1}. \tag{6.10}$$

We note from the Appendix that k can vary from 10^{-3} to 10^3, so Fig. 4 shows a graph of S (as given by (6.10)) *vs.* $\log_{10} k$.

TABLE 2
Parameter values for Fig. 4 and (6.13).

Necessary parameters

Given		*Calculated*	
Parameter	Value	Parameter	Value
B_i	0	μ	$39{\cdot}5k^3$
C_T (mol/cm^3)	10^{-11}	χ	1
$\tilde{D}$ (cm^2/s)	$2{\cdot}8 \times 10^{-7}$		
h (cm)	5×10^{-3}		
L (cm)	$2{\cdot}4 \times 10^{-1}$		
R_T (mol/cm^2)	10^{-12}		
V (cm/s)	1		
x_max	$7{\cdot}92 \times 10^{-1}$		
x_min	$2{\cdot}08 \times 10^{-1}$		

Ancillary parameters

Given		*Calculated*	
Parameter	Value	Parameter	Value
Pe	$3{\cdot}71 \times 10^2$	D	$1{\cdot}34 \times 10^{-4}$
ϵ	$2{\cdot}08 \times 10^{-2}$	D_D	$6{\cdot}95 \times 10^{-3}$

Using the small- and large-μ behaviour of the P function, we can ascertain the large- and small-k behaviour of the graph. For small k, we have

$$S \sim \tilde{k}_\mathrm{on} C_\mathrm{T} \chi, \qquad \tilde{k}_\mathrm{on} \to 0. \tag{6.11}$$

As expected, (6.11) shows that if there is no forward reaction ($\tilde{k}_\mathrm{on} = 0$), the bound concentration will not change ($S = 0$). For large k, we have the following:

$$S \sim \frac{3^{\frac{4}{3}} \chi C_\mathrm{T} V^{\frac{1}{3}} \tilde{D}^{\frac{2}{3}} (x_\mathrm{max}^{\frac{2}{3}} - x_\mathrm{min}^{\frac{2}{3}})}{2^{\frac{1}{3}} (1 - B_\mathrm{i}) \Gamma(\frac{1}{3}) R_\mathrm{T} L^{\frac{1}{3}} h^{\frac{1}{3}} (x_\mathrm{max} - x_\mathrm{min})}, \quad \tilde{k}_\mathrm{on} \to \infty. \tag{6.12}$$

For our choice of parameters in Table 2 and (6.9), the asymptote is given by

$$S \sim 3{\cdot}08 \times 10^{-2}\ \mathrm{s}^{-1}, \quad \tilde{k}_\mathrm{on} \to \infty, \tag{6.13}$$

which is exactly the asymptote plotted in Fig. 4. The presence of a finite asymptote for S in the limit of large $\tilde{k}_\mathrm{on}$ is physically reasonable, since no matter how fast the reaction proceeds, the mass uptake will be limited by the amount of unbound ligand available for assimilation.

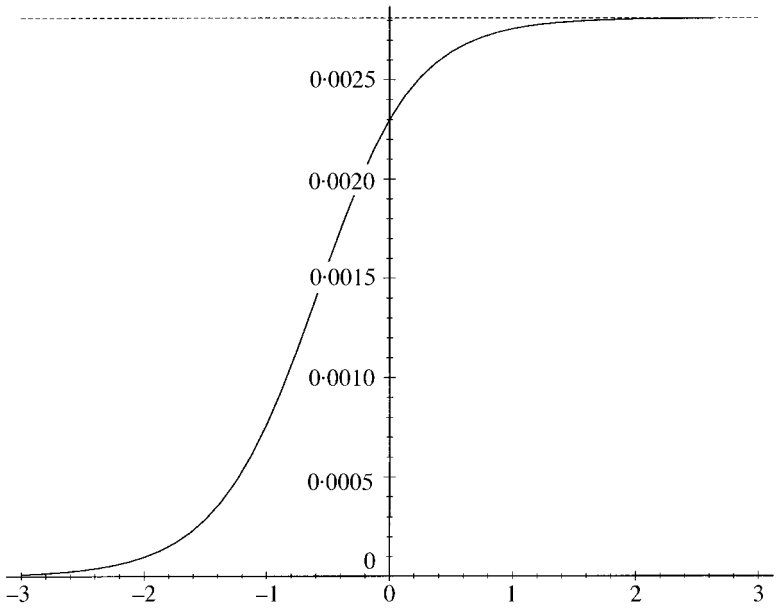

FIG. 4. S *vs.* $\log_{10} k$ as given by (6.10) for the parameters in Table 2, along with the asymptote given in (6.13)

7. Conclusions

In order to further their understanding of chemical and biological systems, scientists must obtain accurate estimates of rate constants for chemical reactions. The advent of SPR technology and its application in the BIAcore^{TM} device have allowed scientists to measure the concentration of bound ligands accurately in real time. Unfortunately, such experimental advances are useless without the necessary mathematical models to interpret the data.

The mathematical model for the system is a convection–diffusion equation with a boundary reaction. By introducing proper dimensionless variables, we determined that there are four separate time-scales associated with the problem. On the convective time-scale t_c, the concentration of unbound ligand in the channel equilibrates, and on the slower diffusive time-scale t_D, the concentration of unbound ligand near the wall equilibrates. Whenever diffusion into the binding surface dominates, the evolution of the bound state evolves on the t_w scale. However, in the more physically realizable case, the evolution of the bound state evolves on the reaction time-scale t.

The key dimensionless group in the problem is the Damköhler number Da. If Da $\ll$ 1, the reaction kinetics decouple from the transport effects. This case is desirable due to the simple form of the solution, and it is the solution to this case which experimentalists have been using to obtain estimates for the rate constants (Corr *et al.* 1994). In (4.15) we established a bound on the velocity such that the kinetics can be considered divorced from transport effects.

For the small Da case, we constructed the next-order correction to the well-known

leading-order solution. This correction, which is $O(\mathrm{Da})$, should provide improved results and an increased range of validity of our expansion. The correction involves an integral of a known quantity, but we obtained explicit closed-form solutions when the initial bound concentration was a constant. The form of the correction suggested a multiple-scale expansion, but the leading-order term of the multiple-scale expansion consists of an infinite series of terms. However, the series converges nicely for $t = o(\mathrm{Da}^{-1})$, and hence a truncated version of the series might be useful.

Unfortunately, with current SPR technology one must often introduce a large number of binding sites in order to get accurate measurements. This increase in R_T can make the threshold in (4.15) difficult to achieve. Therefore, we also analysed the case where $\mathrm{Da} = O(1)$. In this case, the kinetic and transport effects are coupled. We solved for the relevant concentration profile, and thus reduced our system to the nonlinear integrodifferential equation (6.1). One can obtain important data about the rate constants by looking at the small-time asymptotic form of the solution. We indicated how this small-time solution would change as the rate constant varied, and we provided large- and small-$\tilde{k}_\mathrm{on}$ behaviour of the small-time solution.

In addition to providing improved estimates to the rate constants in selected situations, the careful modelling and scaling in Sections 2 and 3 provides a sturdy mathematical framework for further studies. Other areas for further research include dissociation kinetics, the limiting behaviour of small and large K, reactant embedded in a small boundary layer near the channel ceiling rather than on the channel ceiling surface itself, and the consideration of other geometries.

Acknowledgments

This work was performed under National Science Foundation grant DMS-9407531. The author thanks Dr Byron Goldstein for posing the problem and for providing valuable physical insight. The author also thanks Professor Donald S. Cohen for his invaluable contribitions to this paper. Many of the calculations herein were checked with the assistance of MAPLE and MATHEMATICA.

References

BIACORE, INC., undated. *BIAcore*$^{\mathrm{TM}}$ *System Manual* Version 1.1. Uppsala: BIAcore, Inc.

BRODY, J. P., YAGER, R. E., GOLDSTEIN, B., & AUSTIN, R. H. 1996 Biotechnology at low Reynolds number. *Biophys. J.* **71**, 3430–3441.

CHEN, W., KHILKO, S., FECONDO, J., MARGULIES, D. H., & MCCLUSKEY, J. 1994 Determinant selection of major histocompatibility complex class I-restricted antigenic peptides is explained by class I-peptide affinity and is strongly influenced by nondominant anchor residues. *J. Exper. Med.* **180**, 1471–1483.

CORR, M., SLANETZ, A. E., BOYD, L. F., JELONEK, M. T., KHILKO, S., AL-RAMADI, B. K., KIM, Y. S., MAHER, S. E., BOTHWELL, A. L. M., & MARGULIES, D. H. 1994 T cell receptor-MHC class I peptide interactions: affinity, kinetics, and specificity. *Science* **265**, 946–949.

DAVIS, S. J., DAVIES, E. A., BARCLAY, A. N., DAENKE, S., BODIAN, D. L., JONES, E. Y., STUART, D. I., BUTTERS, T. D., DWEK, R. A., & VAN DER MERWE, P. A. 1995 Ligand

binding by the immunoglobulin superfamily recognition molecule CD2 is glycosylation-independent. *J. Biol. Chem.* **270**, 369–375.

EDWARDS, D. A., GOLDSTEIN, B., & COHEN, D. S. Transport effects on surface–volume biological reactions. *J. Math. Bio.* forthcoming.

GLASER, R. 1993 Antigen–antibody binding and mass transport by convection and diffusion to a surface: A two-dimensional computer model of binding and dissociation kinetics. *Anal. Biochem.* **213**, 152–161.

GOLDSTEIN, B., & DEMBO, M. 1995 Approximating the effects of diffusion on reversible reactions at the cell surface: Ligand-receptor kinetics. *Biophys. J.* **68**, 1222–1230.

KARLSSON, R., MICHAELSON, A., & MATTSON, L. 1991 Kinetic analysis of monoclonal antibody–antigen interactions with a new biosensor based analytical system. *J. Immun. Meth.* **145**, 229–40.

KARLSSON, R., ROOS, H., FÄGERSTAM, L., & PERSSON, B. 1994 Kinetic and concentration analysis using BIA technology. *Methods* **6**, 99–110.

LOK, B. K., CHENG, Y.-L., & ROBERTSON, C. R. 1983 Protein adsorption on crosslinked polydimethylsiloxane using total internal reflection fluorescence. *J. Coll. Int. Sci.* **91**, 104–116.

MOTULSKY, H. 1996 *The GraphPad Guide to Analyzing Radioligand Binding Data*. San Diego: GraphPad Software, Inc.

MYSZKA, D. G. 1997 Kinetic analysis of macromolecular interactions using surface plasmon resonance biosensors. *Curr. Opin. Biotech.* **8**, 50–57.

SZABO, A., STOLZ, L., & GRANZOW, R. 1995 Surface plasmon resonance and its use in biomolecular interaction analysis (BIA). *Curr. Opin. Struct. Bio.* **5**, 699–705.

YARMUSH, M. L., PATANKAR, D. B., & YARMUSH, D. M. 1996 An analysis of transport resistance in the operation of BIAcore^{TM}; implications for kinetic studies of biospecific interactions. *Molec. Immun.* **33**, 1203–1214.

Appendix

The BIAcore^{TM} has $L = 2{\cdot}4 \times 10^{-1}$ cm and $h = 5 \times 10^{-3}$ cm. In addition, the SPR detection area is $1{\cdot}4 \times 10^{-1}$ cm long (BIAcore^{TM} System Manual, undated). We assume that the detection area is symmetrically positioned, and thus $x_{\min} = 2{\cdot}08 \times 10^{-1}$ and $x_{\max} = 7{\cdot}92 \times 10^{-1}$.

Many of the physical parameters in the problem vary widely depending on the system under consideration. Tables 3 and 4 provide a listing of values from the literature, as well as the parameters used in this work. Some of the wide variation in parameter sizes can be explained by describing the various studies. For $\tilde{D}$, Yarmush *et al.* (1996) describe the normal range of diffusivities of peptides and proteins. The larger value in Lok *et al.* (1983) is for bovine serum albumin (BSA), and the smaller value for fibrinogen.

While Myszka (1997) gives the range of $\tilde{k}_{\text{off}}$ for which the BIAcore^{TM} provides good results, others provide values for specific reactions. Stable complexes, such as those that result from the binding of a major histocompatibility complex (MHC) class I K^b molecule and a peptide derived from ovalbumin (Chen *et al.* 1994) or the binding between monoclonal antibody 2.3 and BSA (Yarmush *et al.* 1996), have small values for $\tilde{k}_{\text{off}}$. In contrast, the binding between CD2, a T-lymphocyte cell-surface protein, and its ligands (Davis *et al.* 1995) or between MHC with the T-cell receptor and peptide antigens (Corr *et al.* 1994) is quite weak, leading to large values of $\tilde{k}_{\text{off}}$.

TABLE 3
Parameter values from the literature

	Parameter			
Reference	C_T (10^{-11} mol/cm^3)	$\tilde{D}$ (10^{-7} cm^2/s)	$\tilde{k}_{\text{off}}$ (10^{-3} s^{-1})	$\tilde{k}_{\text{on}}$ (10^{8} cm^3/(mol· s))
Chen *et al.* (1994)			$9{\cdot}1 \times 10^{-3} - 1{\cdot}6 \times 10^{-2}$	$6{\cdot}5 \times 10^{-3} - 5{\cdot}9 \times 10^{-2}$
Corr *et al.* (1994)			26	2·1
Davis *et al.* (1995)			160–800	
Lok *et al.* (1983)		8·5		
Ibid.		2·8		
Myszka (1997)			$10^{-3} - 10^{2}$	$10^{-2} - 10^{2}$
Yarmush *et al.* (1996)	0·25–40	4–10	8·9	0·5–50
Used	1	2·8	$10^{-3} - 10^{2}$	$10^{-2} - 10^{4}$
				1

TABLE 4
Parameter values from the literature

	Parameter		
Reference	$\tilde{K}$ (10^{-9} mol/cm^2)	R_T (10^{-12} mol/cm^2)	V (cm/s)
Corr *et al.* (1994)	0·1		
Davis *et al.* (1995)	3–9		1·2–8
Myszka (1997)	$10^{-6} - 10^{2}$		0·4–40
Yarmush *et al.* (1996)		0·25–4	0·36—0·6
Used	n/a	1	1

TABLE 5
Dimensionless parameters

Parameter	**Bound**
Pe	$\geqslant 37{\cdot}4$
D	$\leqslant 2{\cdot}14 \times 10^{-1}$
Da	$\geqslant 2{\cdot}43 \times 10^{-4}$
Da_b	$\geqslant 1{\cdot}33 \times 10^{-4}$
D_D	$\leqslant 1{\cdot}11$
K	$2{\cdot}5 \times 10^{-6} \leqslant K \leqslant 4 \times 10^{4}$

Myszka (1997) indicates that the range of values of $\tilde{k}_{\mathrm{on}}$ he provides for which the BIAcore$^{\mathrm{TM}}$ provides good results can be extended under favorable circumstances. Therefore, we use the moderate value in Subsection 5.3 and the full range in Subsection 6.2.

We use the values from Tables 3 and 4 to calculate our dimensionless parameters. The exact parameters we use are listed in Tables 1 and 2. However, by using extremal values of the dimensional parameters, we can obtain bounds on the dimensionless ones. We note that the bound on Da allows it to be either $o(1)$ or $O(1)$. The bound on D_D is created by using a highly unlikely combinations of extremal values of our parameter. The much more common case is the one quoted in the work, namely that $D_D \ll 1$.